This article has been accepted for publication in a future issue of this journal, but has not been fully edited. Content may change prior to final publication. Citation information: DOI 10.1109/JESTIE.2021.3088387, IEEE Journal of Emerging and Selected Topics in Industrial Electronics

A Nonlinear Backstepping Control Scheme for Rapid Earth Fault Current Limiters in Resonant Grounded Power Distribution Systems: Applications for Mitigating Powerline Bushfires

T. K. Roy, *Member, IEEE*, M. A. Mahmud, *Senior Member, IEEE*, M. A. Barik, *Member, IEEE*, and A. B. M. Nasiruzzaman, *Member, IEEE*, and Amanullah M. T. Oo, *Senior Member, IEEE*

***Abstract*—This work presents a nonlinear backstepping control scheme for rapid earth fault current limiters (REFCLs) in resonant grounded power distribution systems to mitigate the severity of powerline bushfires. The main feature of the proposed control scheme is that it quickly eliminates both active and reactive components of the fault current to make it zero for reducing the chance of igniting bushfires. The nonlinear backstepping control scheme is employed on the dynamical model of a REFCL equipped with a T-type inverter. The desired tracking of the fault current is ensured with the proposed scheme by appropriately injecting the current to the neutral point. The performance of the controller is evaluated in terms of the fault current and faulty phase-to-ground voltage under different fault conditions while following the standard criteria for the practical operation. The fault current compensation capability of the proposed scheme is evaluated for both low and high impedance faults. Simulation results in software and processor-in-loop platforms clearly demonstrate the fault current is limited to a value much lower than its desired value of 0.5 A in less than 1 s which means that the chance of igniting bushfires will be reduced with the proposed controller.**

***Index Terms*—Rapid earth fault current limiters, resonant grounded power distribution system, powerline bushfires, fault current, nonlinear backstepping controller.**

I. Introduction

POWERLINE bushfires start from electric arcs, hot metal particles produced due to the operation of fusees with high current or clashing wires, and vegetation or other combustible particles touching wires with high electric current where all these conditions mostly arise from electric faults [1], [2]. As indicated in [1], bushfires can start instantly from electric faults (mostly, single phase-to-ground) on powerlines (even within 3 ms to 5 ms) and traditional protection schemes are not capable to reduce the fault current within such a time frame for minimizing risks of bushfires. Rapid earth fault current limiters (REFCLs) have the ability to reduce the fault current within few milliseconds and hence, reduce the chance of powerline bushfires. The REFCL is designed using an adjustable inductor (in conjunction with a power electronic converter) which is placed between the neutral point of a substation transformer and ground while having self-adjusting capability to resonate with the total zero sequence capacitance of the distribution system [1]. Therefore, the distribution system becomes a resonant grounded power distribution system (RGPDS) where the REFCL can easily compensate the reactive component of the fault current as it uses an inductor. However, the fault current has both active and reactive components and this current cannot be reduced to zero by eliminating only the reactive component. Furthermore, it is difficult to perfectly tune the inductor with the total zero-sequence capacitance. For this reason, the power electronic converter in the REFCL is used to completely eliminate both active and reactive components of the fault current. Therefore, it is important to design a controller that will be capable to completely reduce the fault current to zero under any fault conditions.

REFCLs are also known as arc suppression devices (ASDs) or ground fault neutralizers (GFNs) and these devices are equipped with the residual current compensator (RCC) inverter [3]. The switching control actions of the RCC inverter play a key role to neutralize the fault current. Different types of proportional integral (PI) controllers are used in [4]–[8] to reduce the fault current in RGPDGs with ASDs and some of these [7], [8] are employed for three-phase ASDs. It is worth mentioning that this paper only considers the control of REFCLs for single-line to ground (SLG) faults which do not require three-phase ASDs and thus, this paper considers only the literature relevant to single-phase ASDs. The main reason for this is that SLG faults are around 70% of the total fault in power distribution systems [1]. A rigorous analysis is presented in [4] to calculate the reference value of the current that needs to be injected through the RCC inverter in an ASD using a PI controller so that the fault current (both active and reactive components) can be completely suppressed. Another PI controller in [5] is designed to suppress only the active component and a similar controller is employed in [6] for suppressing the faulty phase voltage to zero by regulating the zero-sequence voltage. However, all these PI controllers are mostly used for the sinusoidal tracking rather than the regulation of the corresponding neutral voltage or neutral current in the dq-frame and thus, these controllers suffer from poor tracking performance. Moreover, the reference signals for these existing PI controllers are calculated based

T. K.Roy, M. A. Mahmud, A. B. M. Nasiruzzaman, and Amanullah M. T. Oo are with the School of Engineering, Deakin University, Geelong, VIC 3216, Australia. Email: (tkroy, apel.mahmud, nasir.zaman, and aman.m)@deakin.edu.au

T. K. Roy is with the Department of Electronics & Telecommunication Engineering, Rajshahi University of Engineering and Technology, Rajshahi 6204, Bangladesh. Email: tkroy@ete.ruet.ac.bd

M. A. Barik is with the AusNet Services, Melbourne, VIC 3006, Australia. Email: abdul.barik@ausnetservices.com.au

This article has been accepted for publication in a future issue of this journal, but has not been fully edited. Content may change prior to final publication. Citation information: DOI 10.1109/JESTIE.2021.3088387, IEEE Journal of Emerging and Selected Topics in Industrial Electronics

on the thorough analyses of distribution networks.

The tracking performance can be improved and the calculation of the reference current can be simplified using dual-loop control structures where PI controllers can be used in both loops or in conjunction with other controllers such as proportional resonant (PR) controllers. In the dual-loop control structure, an outer voltage control loop and an inner current control loop are used [9], [10], i.e., similar to traditional controllers used to control voltage source inverters (VSIs) [11]. In [9], a lag compensator is used in the outer loop to generate the reference value of the current that needs to be injected to the neutral using the neutral voltage while a PI controller is used for the inner loop to inject the desired current for suppressing the arc due to an SLG fault. Similarly, PI controllers are used in [10] for both loops to serve the similar purpose as discussed in [9]. Though these controllers with the dual-loop structure improve the tracking performance, the damping characteristics are still a major concern as the damping is still limited due to the model-free characteristics of the controllers and their tracking capabilities are severely affected with variations in fault impedances. The combination of PI and PR controllers is proposed in [12] to improve the damping characteristics in a RGPDS where the capacitive current feedback is used to mitigate the overvoltage across the neutral-to-ground due to the asymmetry in distributed parameters and resonance between the arc suppression coil and zero-sequence capacitances. In [12], the output current of the inverter and neutral-to-ground voltage are used to determine the principle for the overvoltage compensation, i.e., to calculate the reference current that will eliminate the arc. However, the gain parameters for the PI+PR controller in [12] need to be selected by satisfying some constraints (e.g., dependencies on the crossover frequencies and other parameters of the system). Another dual-loop controller is presented in [13] for ASDs where PI and PR controllers are combined together for the outer loop while a proportional (P) controller with the inductor current feedback is used for the inner loop. The inductor current feedback in [13] ensures better tracking performance as compared to the capacitive current feedback as presented in [12]. However, the resonant grounding conditions are not considered in [13] and the dynamics of REFCLs are not appropriately captured during the controller design process so far discussed in this work.

A model-based controller is presented in [14] where a finite control set model predictive control scheme is used for a three-phase ASD which has reduced sampling frequency. However, it is not necessary to use a three-phase ASD for suppressing arcs due to an SLG fault. A H_∞ control scheme is proposed in [15] using the first-order model of an ASD. However, the order of the controller in [15] is seventeen which is too high for a first-order system and it is difficult to implement such controllers even after employing a Gram matrix-based order reduction technique as it reduces the order to seven, which is still very high. Another major issue of these controllers is that these use linear model which limit their operations to specific set of operating points (e.g., limited values of the fault impedance, fault on a specific phase, etc.) and all these problems with linear controllers can be overcome using nonlinear control techniques.

Nonlinear backstepping controllers exhibit the properties to ensure the desired tracking of the state variables in a dynamical system [16], [17]. A nonlinear backstepping controller is used in [18] for three-phase ASDs in RGPDSs though it is not essential for most commonly occurring SLG faults. The same backstepping technique is applied in [19] for a single-phase ASD to eliminate the fault current. In [18], [19], the parametric uncertainty is considered for the filter inductance which is then modeled by providing a bound on it. However, the role of this parametric uncertainty is not justified in [18], [19]. Furthermore, a second-order generalized integrator phase-locked loop (SOGI-PLL) with a complicated structure is used and several assumptions are made in [19] to calculate the reference current though the reference current can easily be calculated using the fundamental analytical expression of the neutral current with a faulty phase in a RGPDS. Moreover, the controllers are designed using a full-bridge inverter in which switching losses are high as all these switching devices require high power ratings. Recently, a fast terminal sliding mode controller is designed in [20] for the T-type RCC inverter in a RGPDS to mitigate powerline bushfires by following the operational standard. However, the selection of the sliding surface is difficult and the implementation of this controller requires several differentiators which will introduce additional noises into the system.

The existing literature so far discussed in this paper can be summarized as two broad categories such as model-free and model-based schemes. The model-free controllers exhibit slower response times during transient events in power distribution networks and there are still high chances of igniting fires due to powerline faults. The model-based controllers provide better dynamic responses during the faulted conditions. However, the performance of all these controllers is mostly evaluated for low to moderate impedance faults though the faults in the RGPDS in bushfire prone areas are generally high impedance faults. Therefore, it is essential to further investigate the controller design process by considering all these points.

This paper focuses to design a nonlinear backstepping controller for an RCC inverter in a REFCL using a T-type inverter rather than a conventional full-bridge inverter. The main reason for using the T-type configuration is that some manufacturers of REFCLs (e.g., Siemens) are using it for the RCC inverter. For this T-type configuration, the input DC voltage is splitted into two parts where each part is the half of the total DC voltage and therefore, some of these switches (particularly, switches connected to the neutral point) experience reduced voltage stresses though switches to the upper and lower DC terminals will experience the full DC voltage. The dynamical model of the REFCL is developed by considering the single-phase configuration as it is used for suppressing the fault current for SLG faults in order to reduce the risk of powerline bushfires. The controller is designed by satisfying the Lyapunov stability criteria so that the overall stability of the RGPDS is not affected by the proposed control action. Simulation studies are carried out in the software and processor-in-loop (PIL) platforms with variations in the fault impedances while

This article has been accepted for publication in a future issue of this journal, but has not been fully edited. Content may change prior to final publication. Citation information: DOI 10.1109/JESTIE.2021.3088387, IEEE Journal of Emerging and Selected Topics in Industrial Electronics

applying SLG faults on different phases. Simulation results are also compared with traditional PI and PR controllers which clearly demonstrate the superiority of the proposed scheme in terms of ensuring the standard performance criteria.

II. Modeling of REFCLs

The equivalent circuit of a REFCL is shown in Fig. 1 along with a generalized dual-loop control structure in which an adjustable inductor coil (L_p) is connected between the neutral and ground of the substation. Here, the distribution substation is considered as a balanced one which is supplying power to a three-phase balanced load. Victoria, an Australian state, is the first in the world for applying the REFCL technology for mitigating powerline bushfires [1]. Generally, there are imbalances in distribution networks and the REFCL has high sensitivity to such network imbalances, i.e., it cannot operate if these imbalances exceed a ceratin threshold. Here, this threshold is set by the distribution network companies which is usually 100 mA [1] for the smooth operation of REFCLs. For this reason, the distribution network companies use automatic network balancing techniques for their networks in bushfire prone areas [21]. Therefore, the assumption of the balanced distribution network is practically feasible and it would not affect the accuracy of the controller that will be designed based on this model. A T-type RCC inverter is used with this REFCL for injecting current to the neutral during the fault and this is done by turning on a switch (S_N) as shown in Fig. 1. Generally, S_N is off during the normal operation, i.e., when there is no fault. From Fig. 1, it can be seen that switches connected to the neutral point in the T-type RCC inverter experience the reduced DC voltage, i.e., $V_{dc}/2$ rather than V_{dc} in conventional full-bridge inverters. The input DC voltage for the RCC inverter is constant which is supplied by an auxiliary source. In Fig. 1, the SLG fault is applied on Phase A though this fault may occur on any phases where R_f is the fault resistor and the fault current is I_f. The control objective is to reduce the fault current to zero by injecting current through the RCC inverter at the neutral point. Since L_p makes resonance with the total zero-sequence capacitance of the distribution network, the zero-sequence impedance network corresponding to each phase (which is connected between the phase and ground) is also shown in Fig. 1. In this impedance network for each phase, a resistor (R_0) and capacitor (C_0) are connected parallel where subscripts A, B, and C in these impedance networks denote respective phases, i.e., Phases A, B, and C, respectively which are generalized as $P = \{A,\ B,\ C\}$ for the simplicity in this modeling section. The neutral-to-ground voltage (v_N) in Fig. 1 can be determined as follows:

$$v_N = \frac{v_A + v_B + v_C}{3} \tag{1}$$

where v_A, v_B, and v_C are used to represent phase-to-ground voltages for three phases (i.e., A, B, and C). Applying Kirchhoff's current law (KCL), the current flowing through the neutral can be written as:

$$i_N = i_f + i_{A\sum} + i_{B\sum} + i_{C\sum} \tag{2}$$

where $i_{A\sum}$, $i_{B\sum}$, and $i_{C\sum}$ represent currents through zero sequence impedance networks placed between three phases to the ground. Applying Kirchhoff's voltage law (KVL), the generalized form of the phase-to-ground voltage can be written as:

$$v_P = e_P + v_N \tag{3}$$

where e_P corresponds phase-to-neutral voltages for three phases. The generalized form of the current flowing through the zero sequence impedance networks for each phase can be written as:

$$i_{P\sum} = i_{R_{0P}} + C_{0P}\frac{dv_{C_{0P}}}{dt} = \frac{v_P}{R_0} + C_0\frac{dv_P}{dt} \tag{4}$$

where $i_{R_{0P}}$ is the current through the zero-sequence shunt resistance of the impedance network, $v_{C_{0P}} = v_P$ represents the voltage across the zero-sequence shunt capacitance of the impedance network which is also the phase-to-ground voltage. In this work, it is assumed the RGPDS is balanced for which $R_{0A} = R_{0B} = R_{0C} = R_0$ and $C_{0A} = C_{0B} = C_{0C} = C_0$. It is worth mentioning that the fault detection sensitivity in RGPDSs depends on the balancing condition of the system. Since $v_P = e_P + v_N$ in equation (3), equation (4) can be rewritten as follows:

$$i_{P\sum} = \frac{v_N + e_P}{R_0} + C_0\left(\frac{dv_N}{dt} + \frac{de_P}{dt}\right) \tag{5}$$

Considering $v_f = v_{P'}$ where $v_{P'}$ represents the phase-to-ground voltage for the faulty phase and the SLG fault may occur on any phases. With this, the fault current can be written as:

$$i_f = \frac{v_f}{R_f} = \frac{v_{P'}}{R_f} \tag{6}$$

In Fig. 1, the fault is applied on Phase A and hence, $v_{P'} = v_A$ where the subscript of the voltage will change depending on the faulty phase. This means that $v_{P'}$ will be v_B or v_C if the SLG fault occurs on Phase B or Phase C, respectively. Using equations (5)–(6) and considering $e_A + e_B + e_C = 0$ for a balanced system, equation (2) can be simplified as:

$$i_N = \frac{v_{P'}}{R_f} + \frac{3v_N}{R_0} + 3C_0\frac{dv_N}{dt} \tag{7}$$

Depending on the faulty phase, v_N can be expressed as follows:

$$v_N = v_{P'} - e_{P'} \tag{8}$$

where $e_{P'}$ is the phase-to-neutral voltage for the faulty phase. For example, $e_{P'} = e_A$ if the SLG fault occurs on Phase A as shown in Fig. 1. Similarly, $e_{P'}$ will be e_B or e_C if the SLG fault occurs on Phase B or Phase C, respectively. Using equation (8), equation (7) can be written as follows:

$$\begin{aligned} i_N = &\left(\frac{3}{R_0} + \frac{1}{R_f}\right)v_{P'} + 3C_0\frac{dv_{P'}}{dt} \\ &- \left(\frac{3}{R_0}e_{P'} + 3C_0\frac{de_{P'}}{dt}\right) \end{aligned} \tag{9}$$

The aim of developing the model of the REFCL in this section is to design controller that will eliminate the fault current in order to reduce the risk of powerline bushfires.

This article has been accepted for publication in a future issue of this journal, but has not been fully edited. Content may change prior to final publication. Citation information: DOI 10.1109/JESTIE.2021.3088387, IEEE Journal of Emerging and Selected Topics in Industrial Electronics

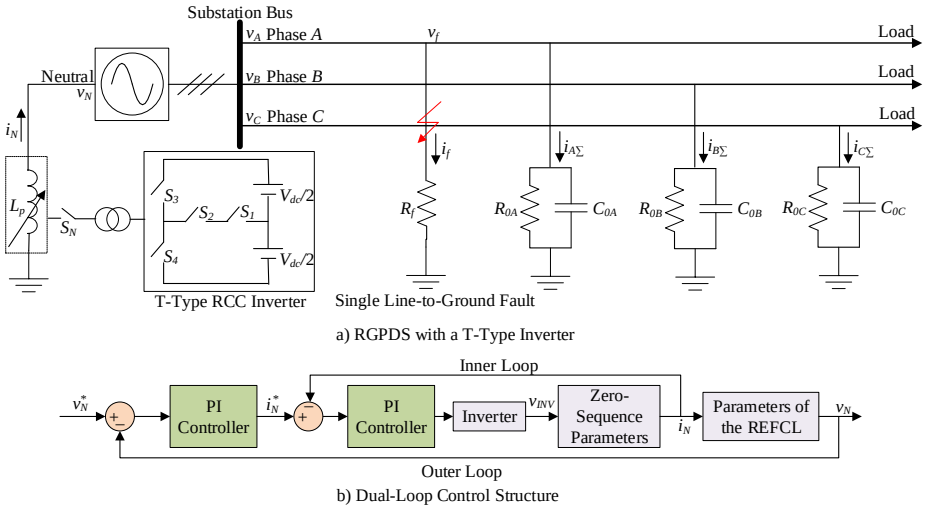

Fig. 1. A REFCL with a T-type RCC inverter connected to a power distribution substation with a dual-loop controller

Based on equation (9), this will be possible if the reference current is selected as follows [19]:

$$i_{N_{ref}} = -\left(\frac{3}{R_0}e_{P'} + 3C_0\frac{de_{P'}}{dt}\right) \tag{10}$$

By applying KVL between the neutral and ground where the REFCL is connected, it can be simplified as:

$$\frac{di_N}{dt} = \frac{mV_{dc} - v_N}{L_p} \tag{11}$$

where m is the modulation index of the RCC inverter. The generalized nonlinear form of equation (11) can be expressed as:

$$\dot{x} = f(x) + g(x)u \tag{12}$$

with $x = i_N$, $f(x) = -\frac{v_N}{L_p}$, $g(x) = \frac{V_{dc}}{L_p}$, and $u = m$. The backstepping controller needs to be designed based on the model as presented by equation (12) so that i_N is tracked to its reference value in equation (10) and the detailed controller design process for the REFCL is discussed in the following section.

III. Nonlinear Backstepping Controller Design for REFCLs

In this section, the proposed scheme is designed for a simple system which can easily be expanded to large distribution networks with multiple units. The model of REFCLs in Section II can be represented in the decoupled from with respect to the buses where these are connected. Hence, the proposed controller can be designed in a decentralized way for the RGPDS with multiple REFCLs. In the proposed nonlinear backstepping control scheme, the control law (u) is obtained in such a way that the desired tracking performance for the neutral current is ensured. Hence, the design process starts with the tracking error (e) and this tracking error for the neutral current can be defined as follows:

$$e = x - x_d \tag{13}$$

where $x_d = i_{N_{ref}}$ is the desired or reference value. Now. it is essential to analyze the dynamic characteristics of this error in order to ensure the convergence of e towards zero and the dynamic of e can be obtained as follows:

$$\dot{e} = \dot{x} - \dot{x}_d = f(x) + g(x)u - \dot{x}_d \tag{14}$$

The convergence of the error is generally analyzed using the Lyapunov stability theory where the energy of the system is either positive definite ($W > 0$) or positive semi-definite ($W \geq 0$). Here, this energy function is defined in terms of the error variable which can be written as:

$$W = \frac{1}{2}e^2 \tag{15}$$

where W is positive definite or positive semi-definite for any values of e. This energy function is also known as the control Lyapunov function (CLF) and the derivative of W should be negative definite or negative semi-definite (i.e., $\dot{W} < 0$ or $\dot{W} \leq 0$, respectively) in order to ensure the convergence of e towards zero and make the system stable. Hence, the control signal u for the RCC inverter in the REFCL needs to be obtained in a way that the system becomes stable. For this purpose, $\dot{W}$ can be written as:

$$\dot{W} = e\dot{e} = e\left[f(x) + g(x)u - \dot{x}_d\right] \tag{16}$$

The RGPDS with the REFCL will satisfy the stability criteria for any values of e including $e = 0$, i.e., $\dot{W} \leq 0$ if and only if the following condition is satisfied:

$$f(x) + g(x)u - \dot{x}_d = -ke \tag{17}$$

where $k > 0$ is a positive gain of the controller that defines the convergence speed of the error towards zero. Using equation (17), the control input can be obtained as:

$$u = -\frac{1}{g(x)}\left(f(x) - \dot{x}_d + ke\right) = \frac{v_N + L_p(\dot{x}_d - ke)}{V_{dc}} \tag{18}$$

with

$$\dot{x}_d = -\left(\frac{3}{R_0}\frac{de_{P'}}{dt} + 3C_0\frac{d^2e_{P'}}{dt^2}\right) \tag{19}$$

For the control input in equation (18), equation (16) can be written as:

$$\dot{W} = -ke^2 \leq 0 \tag{20}$$

This article has been accepted for publication in a future issue of this journal, but has not been fully edited. Content may change prior to final publication. Citation information: DOI 10.1109/JESTIE.2021.3088387, IEEE Journal of Emerging and Selected Topics in Industrial Electronics

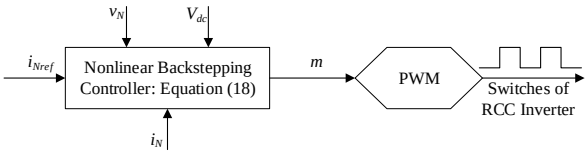

Fig. 2. The implementation block diagram of the designed controller for the RCC inverter in a REFCL

TABLE I
SIMULATION PARAMETERS

Parameters	values
Inductor Coil (L_p)	0.9 H
Zero Sequence Resistance (R_0)	28 kΩ
Zero Sequence Capacitance (C_0)	4 μF
Fault Resistance (R_f)	350 Ω $\sim$ 26 kΩ
Nominal Load Resistance per Phase	400 Ω
Phase-to-Neutral Voltage (E_P)	12.7 kV(rms)
Phase-to-Ground Voltage (v_P)	12.7 kV(rms)
Line-to-Line Voltage	22 kV(rms)
DC Voltage (V_{dc}/2)	400 V
Controller Gain (k)	20,000
Switching Frequency (f_s)	10 kHz

which indicates the stability of the system for any values of e. Hence, equation (18) can be used for minimizing the fault current in a RGPDS. The implementation block diagram of the designed controller is shown in Fig. 2 from where it can be seen that the control law is formed using equation (18) where the reference value of the current is determined from equation (10). The values of V_{dc} and L_p are known in equation (18) while v_N and i_N are measured from the system as shown in Fig. 1. This means that the controller uses the sensor measurement of the phase-to-neutral voltage of the faulty phase, i.e., e'_P to calculate $i_{N_{ref}}$. Other sensor measurements include v_N, V_{dc}, and i_N. It is also worth mentioning that the proposed control scheme can also be implemented on conventional voltage source converters (VSCs) without any modification as the fundamental principle of VSCs and T-type inverter is same. Furthermore, the mathematical model for both T-type inverters and VSCs is similar after applying the averaging technique [22], [23]. Moreover, the proposed scheme can easily be implemented on three-phase ASDs without any modifications while carrying out the similar analysis as the model in Section II is derived by considering a balanced distribution system and a single-phase and three-phase balanced systems are same when these are transformed into the dq-frame. Please note that the analysis associated with the backstepping controller is carried out off-line and the control signal is then used for controlling the REFCL through the RCC inverter, i.e., only equation (18) as shown in Fig. 2 is used during the implementation process. Hence, the practical implementation does not require all these step-by-step calculations. Finally, the switching control input is obtained using equation (18) and a pulse width modulation (PWM) scheme is then employed to determine the pulses for switches in the T-type inverter. This controller is applied on the system in Fig. 1 and its performance is analyzed through simulation results as discussed in the following section.

IV. CONTROLLER PERFORMANCE EVALUATION

A RGPDS as shown in Fig. 1 is used to evaluate the performance of the designed nonlinear backstepping controller (NBC) by considering different operating conditions. The parameters used for the simulation studies in this section are provided in Table I where these parameters are considered based on the Victorian power distribution networks in the bushfire prone area. The simulation studies are carried out in MATLAB/SIMULINK with variations in fault resistance and unbalances in the load demand. The simulation results are analyzed based on the practical operational standard as presented in [24] where several criteria are set for the phase-to-ground voltage of the faulty phase and the neutral current with respect to time. For example, the faulty phase-to-ground voltage should be maintained at 250 V using the REFCL within 2 s in order to reduce the risk of powerline bushfires for both low and high fault resistances [24]. It is worth mentioning that value of the low fault resistance is considered as any value of R_f below 1 kΩ while for high impedance fault this value would be higher than 1 kΩ. However, it is expected that the REFCL has the ability to detect an SLG fault with the fault resistance up to 25.4 kΩ to mitigate powerline bushfires [24]. Therefore, the simulation in this section is carried out by considering the highest value of the fault resistance as 26 kΩ and the lowest as 350 Ω. For the low impedance faults, the faulty phase-to-ground voltage needs to be checked at 85 ms and 0.5 s in addition to 2 s as mentioned earlier on. Hence, after applying the REFCL (which is generally done at the instance of detecting the SLG fault), the values of the faulty phase-to-ground voltage should be maintained at 1900 V and 750 V within 85 ms and 0.5 s, respectively [24]. Moreover, the value of the neutral current should be kept below 0.5 A within these timescale after applying the REFCL [24]. Hence, the performance of the designed controller needs to be assessed in terms of the phase-to-ground voltage of the faulty phase and the current flowing through neutral which has been done in this section. It is worth mentioning that the operation of the RCC inverter relies on the fault detection algorithm and REFCLs are capable to detect SLG faults almost instantly. In this work, it is considered that the fault is detected by the REFCL through an algorithm (e.g., as presented in [25]) and hence, the fault detection is considered as the out of scope of this work though the proposed scheme can be implemented with such an algorithm. In [25], the fault is detected within 3 ms to 6 ms after the occurrence. The following two cases are considered to analyze the performance of the controller through simulation results:

- Variations in the fault resistance with an SLG fault on Phase B and
- Unbalances in loads along with variations in the fault resistance considering an SLG fault on Phase C

For both cases, the fault is applied at t=0.5 s and the REFCL operation is also initiated at the same instant, i.e., t=0.5 s. The performance of the designed controller is compared with a PI controller as proposed in [6] and a PR controller in [12]. An additional case study is presented to demonstrate the performance of the controller through the PIL simulation.

This article has been accepted for publication in a future issue of this journal, but has not been fully edited. Content may change prior to final publication. Citation information: DOI 10.1109/JESTIE.2021.3088387, IEEE Journal of Emerging and Selected Topics in Industrial Electronics

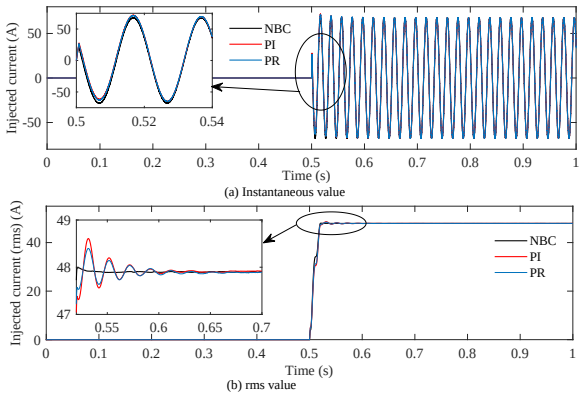

Fig. 3. Current injected to the neutral by the RCC inverter for R_f=350 Ω when an SLG fault is applied on Phase B and the load is balanced

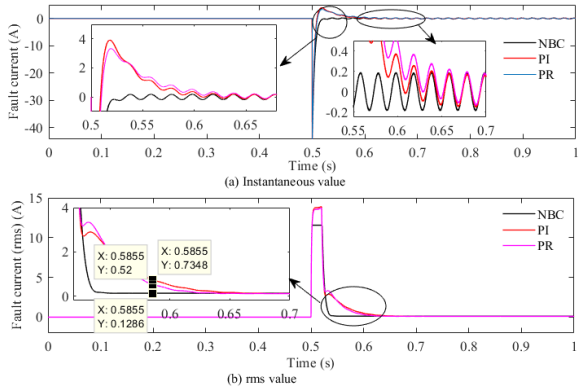

Fig. 4. Fault current for R_f=350 Ω when an SLG fault is applied on Phase B and the load is balanced

- **Case 1:** Controller performance evaluations with variations in the fault resistance for an SLG fault on Phase B

For this case study, an SLG fault is applied on Phase B and the REFCL easily detects the fault through its inherent fault detection algorithm. It is worth to note that the fault detection is out of the scope of this paper as the main focuses of this work are to design and implement the controller for the RCC inverter. The system in Fig. 1 is simulated by considering two different fault resistances (one for low and one for high resistances) as indicated earlier on while considering the load as balanced. The simulation studies are carried out for the values of R_f as 350 Ω and 16 kΩ. The instantaneous and rms values of the current injected to the neutral by the RCC inverter, fault current, and phase-to-ground fault voltage are shown in Figs. 3, 4, and 5, respectively when the value of R_f is 350 Ω. From Fig. 3, it can be seen that the current injected by the RCC inverter is zero before t=0.5 s, i.e., before applying the SLG fault on Phase B. However, the RCC inverter is activated at the instance of occurring the fault and it starts injecting the current as shown in Fig. 3. The currents injected by the RCC inverter with the designed NBC, PI, and PR controllers are shown in Fig 3. However, it is hard to distinguish the difference from the instantaneous value as shown in Fig. 3(a). The rms value of the injected current in Fig. 3(b) shows that the designed controller almost instantly injected the desired current while the PI and PR controllers take around 0.1 s for injecting the current which is sufficient to ignite fire. The fault current in Fig. 4 quickly reduces to zero when the NBC is used while it takes some times for both PI and PR controllers. Furthermore, the fault current is well below 0.5 A with the designed controller though it is higher at the beginning with PI and PR controllers. The rms value of the fault current in Fig. 4(b) clearly shows that the settling time of the designed controller is much faster than that of PI and PR controllers. The phase-to-ground voltage for the faulty phase, i.e., Phase B is shown in Fig. 5. From this figure, it can be seen that the value of this phase-to-ground voltage is 12.7 kV(rms) before t=0.5 s, i.e., before applying the fault. During the fault, this voltage should be reduced to a lower value according to the practical operational standard as discussed earlier on. Since the fault is a low impedance fault, the value of the faulty phase-to-ground needs to be unreserved at 85 ms, 0.5 s, and 2 s after utilizing the REFCL. As per the operational standard as indicated in [24], the value of this voltage should be 1900 V within 85 ms after applying the REFCL. Since the fault is applied at t=0.5 s, the phase-to-ground voltage of Phase B needs to be unreserved at t=0.585 s. From Fig. 5(b), it can be seen that the value of the phase-to-ground voltage with the designed controller is around 45 V whereas it is around 185 V with the traditional PI controller and around 259 V with the PR controller. Though all three controllers maintain the standard operational criteria, the value of the phase-to-ground voltage is much lower when the designed NBC is used. Furthermore, the value of this phase-to-ground voltage with all these controllers becomes lower than 40 V within 0.2 s after applying the REFCL, i.e., at t=0.7 s as indicated in Fig. 5. Hence, it is not essential to observe the faulty phase-to-ground voltage at t=1 s and t=2.5 s, i.e., after 0.5 s and 2 s of activating the REFCL.

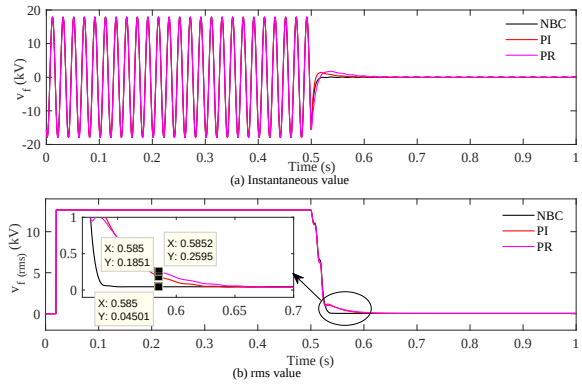

Fig. 5. Faulty phase-to-ground voltage for R_f=350 Ω when an SLG fault is applied on Phase B and the load is balanced

The simulation is also carried out for a high impedance fault where the value of the fault resistance is considered as 16 kΩ and the similar responses (i.e., the current injected by the RCC inverter, fault current, and faulty phase-to-ground voltage) are considered to analyze the performance. The rms values of the faulty phase voltage is shown in Table II which clearly show that all controllers perform well after 0.5 s of occurring the fault. However, the NBC performs better than other controllers at the instant of 85 ms after applying the fault. The rms values of the faulty

This article has been accepted for publication in a future issue of this journal, but has not been fully edited. Content may change prior to final publication. Citation information: DOI 10.1109/JESTIE.2021.3088387, IEEE Journal of Emerging and Selected Topics in Industrial Electronics

TABLE II
THE RMS VALUES OF THE FAULTY PHASE VOLTAGE AT THE CRITICAL TIME INSTANTS FOR R_f=16 kΩ

RCC activation time	Simulation time	PI	PR	NBC
85 ms	0.585 s	0.887 kV	1.808 kV	0.4323 kV
0.5 s	1 s	0.4323 kV	0.4323 kV	0.4323 kV
2 s	2.5 s	0.4323 kV	0.4323 kV	0.4323 kV

TABLE III
THE RMS VALUES OF THE FAULTY PHASE CURRENT AT THE CRITICAL TIME INSTANTS FOR R_f=16 kΩ

RCC activation time	Simulation time	PI	PR	NBC
85 ms	0.585 s	0.351 A	0.1174 A	0.1174 A
0.5 s	1 s	0.0138 A	0.0041 A	0.0041 A
2 s	2.5 s	0.0138 A	0.0041 A	0.0041 A

phase current at different critical time instants (i.e., at 85 ms, 0.5 s, and 2 s after the fault occurrence) are shown in Table III. From this table, it can be found the designed NBC and PR controllers compensate the fault current almost in a similar manner and perform better than the PI controller. Moreover, the PI controller takes around 0.1 s to inject the desired current when R_f=16 kΩ.

- **Case 2:** Controller performance evaluations with variations in the fault resistance for an SLG fault on Phase C and unbalanced load conditions

In this case study, the SLG fault is applied on Phase C at t=0.5 s and the load is considered as unbalanced to analyze the effectiveness of the designed controller under different operating conditions. The performance of the designed controller is analyzed by considering both low and high values of the fault resistance. As discussed in the previous case study, the performance of the controller is analyzed in terms of the current injection capability of the RCC inverter, overall fault current elimination capability, and reduction in the phase-to-ground voltage of the faulty phase. At the first instance, the simulation is carried out by considering the value of R_f as 850 Ω. The current injected by the RCC inverter is shown in Fig. 6 from where it can be clearly seen that all controllers start injecting current

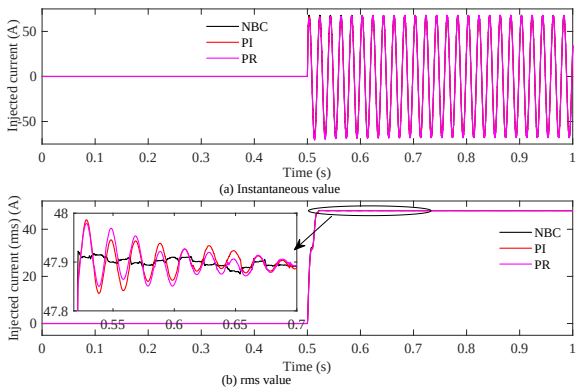

Fig. 6. Current injected to the neutral by the RCC inverter for R_f=850 Ω when an SLG fault is applied on Phase C and the load is unbalanced

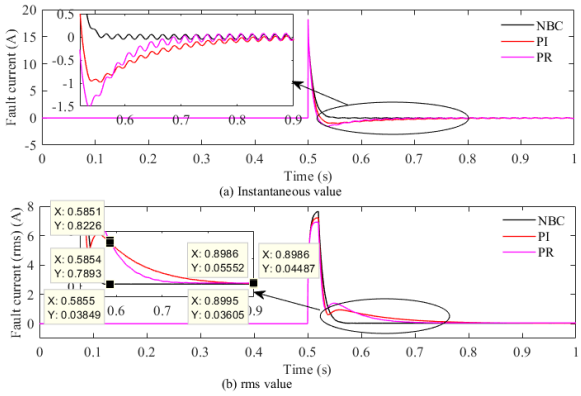

Fig. 7. Fault current for R_f=850 Ω when an SLG fault is applied on Phase C and the load is unbalanced

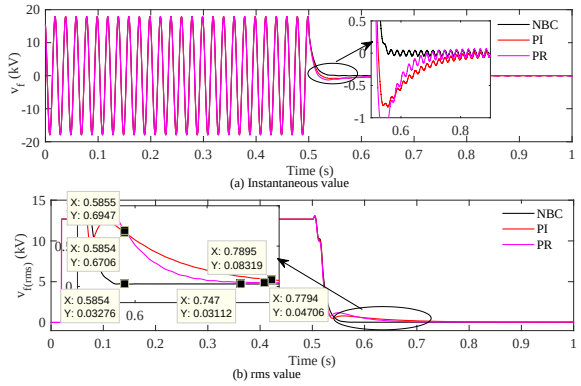

Fig. 8. Faulty phase-to-ground voltage for R_f=850 Ω when an SLG fault is applied on Phase C and the load is unbalanced

at t=0.5 s, i.e., when the SLG fault occurs on Phase C. However, the REFCL with PI and PR controllers take some times to ensure the injection of the desired current to the neutral. On the other hand, the designed NBC appropriately injects the desired current for compensating the fault current which is evident from Fig. 7. The fault current as shown in Fig. 7 quickly settles down to zero when the RCC inverter within the REFCL uses the designed controller. From Fig. 7(b), it can be seen that the PI controller takes around 0.3 s to completely eliminate the fault current and this timeframe is enough to ignite the fire which is not the case for the NBC as it keeps the fault current within the standard operating criteria. In this condition, the phase-to-ground voltage for the faulty phase is shown in Fig. 8 from where it can be seen that this value is much higher for PI and PR controllers while comparing with the NBC though all controllers maintain the operational standard. The unbalanced loading conditions slightly affect the current injection with all controllers where the PI controller is more sensitive to these unbalances than the designed NBC.

The performance of the designed controller is also evaluated by considering a very high fault impedance where the value of the R_f is considered as 26 kΩ. This value is considered as it is the highest for which the REFCL is capable to detect the SLG fault in an RGPDS. The similar fault condition is considered, i.e., the fault is applied on Phase C at t=0.5 s and the REFCL is also placed into operation at the same instant. The current compensation

This article has been accepted for publication in a future issue of this journal, but has not been fully edited. Content may change prior to final publication. Citation information: DOI 10.1109/JESTIE.2021.3088387, IEEE Journal of Emerging and Selected Topics in Industrial Electronics

TABLE IV
THE RMS VALUES OF THE FAULTY PHASE VOLTAGE AT THE CRITICAL TIME INSTANTS FOR R_f=26 KΩ

RCC activation time	Simulation time	PI	PR	NBC
85 ms	0.585 s	2.17 kV	2.276 kV	0.3176 kV
0.5 s	1 s	1.3 kV	0.983 kV	0.4403 kV
2 s	2.5 s	1.3 kV	0.98 kV	0.4403 kV

TABLE V
THE RMS VALUES OF THE FAULTY PHASE CURRENT AT THE CRITICAL TIME INSTANTS FOR R_f=16 KΩ

RCC activation time	Simulation time	PI	PR	NBC
85 ms	0.585 s	0.1641 A	0.0848 A	0.0461 A
0.5 s	1 s	0.0441 A	0.0239 A	0.0023 A
2 s	2.5 s	0.0441 A	0.0239 A	0.0023 A

capability of the RCC inverter in the REFCL is shown through the rms values of the faulty phase and fault current as depicted in Table IV and Table V, respectively. From both tables, it can be seen that the NBC outperforms both PI and PR controllers for all time instants.

- **Case 3:** Controller performance evaluation through the PIL simulation

The application of the designed NBC on a practical system is evaluated through the PIL simulation. The main concept of the PIL simulation is that the newly developed control algorithm will run in an external processor where the original system model will be a simulation platform rather than a real hardware. Results for such simulations are acceptable, especially for verifying the control algorithm. As an interfacing block between the software and processor is used to generate the C code which is then deployed on the processor. The process finally generates the control signal and send it to the original system through the same interfacing unit. Such simulations are widely acceptable as it is equivalent to any other real-time simulation in terms of verifying the newly developed algorithms or methods. In this PIL simulation, the newly developed control signal is developed in the MATLAB/SIMULINK platform as shown in Fig. 9. Here, the control signal is developed based on the equation derived for the control input. Similarly, the

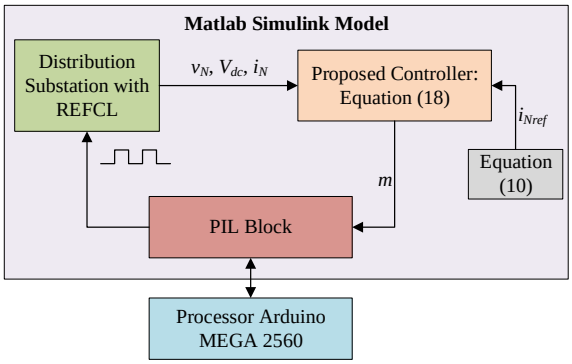

Fig. 9. Signal flow diagram for the PIL simulation

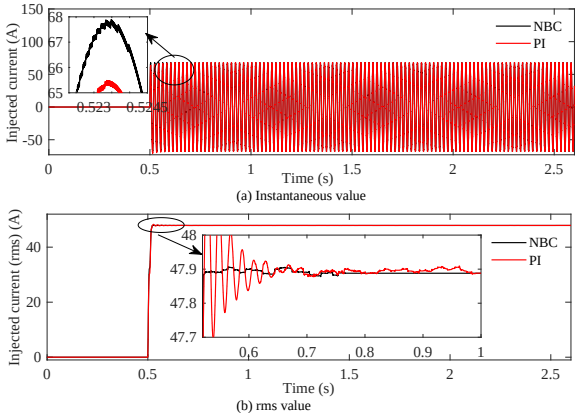

Fig. 10. Injected current from the PIL simulation for R_f=350 Ω when an SLG fault is applied on Phase C under the balanced loading condition

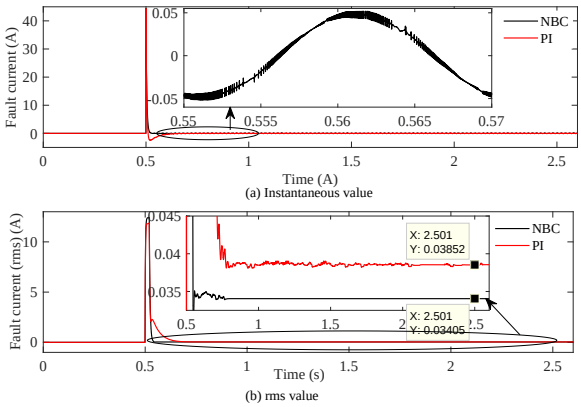

Fig. 11. Fault current from the PIL simulation for R_f=350 Ω when an SLG fault is applied on Phase C under the balanced loading condition

reference signal for the controller is determined in the simulation platform. The newly developed control signal is then fed to the PIL block which works as an interfacing unit between the Arduino MEGA 2560 processor and system model in the simulation platform. Finally, the control signal is deployed in the processor and sent it back to the simulation platform through this PIL block. The output of the PIL block is then fed to the original system. The same system, as discussed earlier in this section, is used in the MATLAB/SIMULINK platform and the PIL simulation is

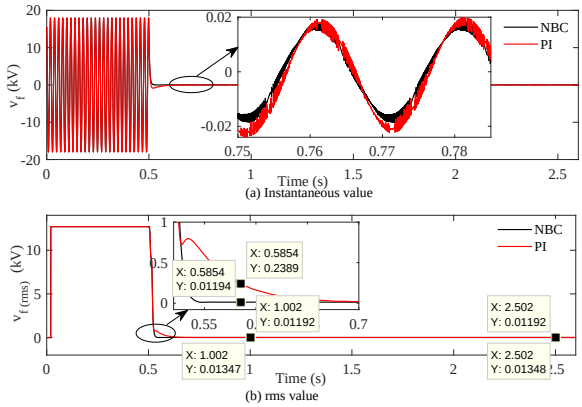

Fig. 12. Faulty phase-to-ground voltage from the PIL simulation for R_f=350 Ω when an SLG fault is applied on Phase C under the balanced loading condition

This article has been accepted for publication in a future issue of this journal, but has not been fully edited. Content may change prior to final publication. Citation information: DOI 10.1109/JESTIE.2021.3088387, IEEE Journal of Emerging and Selected Topics in Industrial Electronics

carried out for R_f =350 Ω while considering the similar fault sequence, i.e., the fault is applied at t=0.5 s and the RCC inverter is activated at the same instant. However, the fault is now applied on Phase C instead of Phase B to verify the practicality for other phases. Different responses such as the current injected to the neutral by the RCC inverter, fault current, and faulty phase voltage are shown in Fig. 10 to Fig. 12 under the balanced loading conditions. All these responses satisfy the operational standard required for mitigating the powerline bushfires. The only difference between the software and PIL simulation is that the waveforms are less smooth for the results obtained from the PI simulation. However, the designed NBC works perfectly and achieves the desired control objectives. It is worth mentioning that the processing speed for this processor is less than 10 μs. This is probably due to the smaller number of variables associate with the control input. Therefore, it is practically feasible to implement on real-world power distribution networks.

From all these results, it can be seen that the NBC has better transient responses (please refer to the black line in zoomed windows in Fig. 3 to Fig. 8 and Fig. 10 to Fig. 12) while comparing with the PI controller (please refer to the red line in respective figures). The main reason behind better transient responses with the designed NBC is that the existing control loops are replaced with a back-stepping control law along with a feedforward term. The designed NBC ensures better steady-steady performance within timeframe of 2 s after occurring the fault while comparing with the PI controller. It is also worth noting that the PI controller in [6] uses a sinusoidal reference for there are some tracking errors. The results with the PR controller shows some improvements over the PI controller but the NBC still outperforms both PI and PR controllers. Furthermore, the NBC ensures faster settling time than the PI controller where the difference can be seen at the first few milliseconds which play a key role to mitigate powerline bushfires.

V. Conclusions

A nonlinear backstepping controller is designed for the residual current compensator inverter in a rapid earth fault current limiter in a resonant grounded power distribution system. The switching control input of the residual current compensator inverter is determined in a way that the fault current is quickly eliminated so that the risk of powerline bushfires is mitigated. At the same time, the overall stability of the system is ensured which is proven through the control Lyapunov function. The performance of the designed controller is evaluated through rigorous simulation studies by considering different operating conditions (mainly, with variations in the fault resistance under balanced and unbalanced loading conditions). Simulation results under all operating scenarios clearly demonstrate that the designed nonlinear backstepping controller ensures the injection of the desired current through the residual current compensator inverter. Hence, the fault current is effectively reduced to a value lower than the operational threshold of 0.5 A. Moreover, the designed nonlinear back-stepping controller maintains the phase-to-ground voltage of the faulty phase to a much lower value that is required to ensure the practical operational standard. Simulation results also demonstrate the designed controller performs much better than the proportional integral controller in terms of both tracking error and settling time under both balanced and unbalanced loading conditions with variations in the fault resistance. The implementation of the designed controller requires to know the exact value of the inductor for the arc suppression coil which is one of the major limitations and the performance of this controller will be severely affected with variations in parameters. This parameter sensitivity issue can be overcome by estimating relevant parameters through adaptation laws in the adaptive controller which is planned as a future work. Future works will also devote into the consideration of the fault detection algorithm during the implementation of the controller.

References

[1] T. Orton, "Powerline Bushfire Safety Taskforce: Final Report," *Energy Safe Victoria*, September 2011.

[2] B. Teague, R. McLeod, and S. Pascoe, "2009 Victorian Bushfires Royal Commission," *Parliament of Victoria*, July 2010.

[3] K. M. Winter, "The RCC ground fault neutralizer–a novel scheme for fast earth-fault protection," in *CIRED 2005 - 18th International Conference and Exhibition on Electricity Distribution*, 2005, pp. 1–4.

[4] A. Gargoom, M. A. Barik, M. A. Mahmud, M. E. Haque, A. M. T. Oo, H. Al-Khalidi, and M. Cavanagh, "Residual current compensator based on voltage source converter for compensated distribution networks," in *2018 IEEE Power Energy Society General Meeting (PESGM)*, 2018, pp. 1–5.

[5] M. Janssen, S. Kraemer, R. Schmidt, and K. Winter, "Residual current compensation (RCC) for resonant grounded transmission systems using high performance voltage source inverter," in *2003 IEEE PES Transmission and Distribution Conference and Exposition (IEEE Cat. No.03CH37495)*, vol. 2, 2003, pp. 574–578 vol.2.

[6] M. Qi, H. Leng, Z. Zhang, L. Yang, S. Peng, and X. Zeng, "Fast disposal method for reducing electricity risk of single-phase ground fault in distribution network," in *2017 China International Electrical and Energy Conference (CIEEC)*, 2017, pp. 554–558.

[7] Z.-Y. Zheng, M.-F. Guo, N.-C. Yang, and T. Jin, "Flexible arc-suppression method based on improved distributed commutations modulation for distribution networks," *International Journal of Electrical Power & Energy Systems*, vol. 116, p. 105580, 2020.

[8] Fangyao Wang, Moufa Guo, and G. Yang, "Novel arc-suppression methods based on cascaded H-bridge converter," in *2016 Asia-Pacific International Symposium on Electromagnetic Compatibility (APEMC)*, vol. 01, 2016, pp. 691–694.

[9] D. Chen, X. Zeng, S. Peng, Y. Wang, Y. Wang, Y. Zhao, and X. Liu, "Active inverter device with double closed loop control method for arc suppression in distribution network," in *2017 China International Electrical and Energy Conference (CIEEC)*, 2017, pp. 549–553.

[10] Wen Wang, Lingjie Yan, Bishuang Fan, and Xiangjun Zeng, "Control method of an arc suppression device based on single-phase inverter," in *2016 International Symposium on Power Electronics, Electrical Drives, Automation and Motion (SPEEDAM)*, 2016, pp. 929–934.

[11] T. K. Roy, M. A. Mahmud, W. X. Shen, and M. E. Haque, "Robust direct power control of grid-connected photovoltaic systems based on adaptive partial feedback linearization," in *2017 12th IEEE Conference on Industrial Electronics and Applications (ICIEA)*, 2017, pp. 64–69.

[12] W. Wang, L. Yan, X. Zeng, B. Fan, and J. M. Guerrero, "Principle and design of a single-phase inverter-based grounding system for neutral-to-ground voltage compensation in distribution networks," *IEEE Transactions on Industrial Electronics*, vol. 64, no. 2, pp. 1204–1213, 2017.

[13] W. Wang, X. Zeng, L. Yan, X. Xu, and J. M. Guerrero, "Principle and control design of active ground-fault arc suppression device for full compensation of ground current," *IEEE Transactions on Industrial Electronics*, vol. 64, no. 6, pp. 4561–4570, 2017.

[14] W. Qiu, M. Guo, G. Yang, and Z. Zheng, "Model-predictive-control-based flexible arc-suppression method for earth fault in distribution networks," *IEEE Access*, vol. 7, pp. 16 051–16 065, 2019.

[15] Y. Qu, W. Tan, and Y. Yang, "H-infinity control theory apply to new type arc-suppression coil system," in *2007 7th International Conference on Power Electronics and Drive Systems*, 2007, pp. 1753–1757.

[16] T. K. Roy and M. A. Mahmud, "Dynamic stability analysis of hybrid islanded DC microgrids using a nonlinear backstepping approach," *IEEE Systems Journal*, vol. 12, no. 4, pp. 3120–3130, 2018.

[17] T. K. Roy, M. A. Mahmud, and A. M. T. Oo, "Operations of DC microgrids in coordination with AC grids based on nonlinear backstepping controllers," in *2018 IEEE Power Energy Society General Meeting (PESGM)*, 2018, pp. 1–5.

[18] Z. Zheng, M. Guo, N. Yang, and T. Jin, "FASD based on BSC method for distribution networks," *IET Generation, Transmission Distribution*, vol. 13, no. 24, pp. 5487–5494, 2019.

[19] Z.-Y. Zheng, M.-F. Guo, N.-C. Yang, and T. Jin, "Single-phase flexible arc suppression device based on BSC-SOGI-PLL method for distribution networks," *International Journal of Electrical Power & Energy Systems*, vol. 121, p. 106100, 2020.

[20] T. K. Roy, M. A. Mahmud, M. A. Barik, A. B. M. Nasiruzzaman, and A. M. T. Oo, "A non-singular fast terminal sliding mode control scheme for residual current compensation inverters in compensated distribution networks to mitigate powerline bushfires," *IET Generation, Transmission & Distribution*, vol. Early Access, DOI: 10.1049/gtd2.12110, 2021.

[21] M. A. Barik, A. Gargoom, M. A. Mahmud, M. E. Haque, M. Cavanagh, H. Al-Khalidi, and A. M. T. Oo, "Automatic network capacitive balancing technique for resonant grounded power distribution systems," *IET Generation, Transmission & Distribution*, vol. Early Access, DOI: 10.1049/iet-gtd.2020.0937, 2020.

[22] M. Barzegar-Kalashani, B. Tousi, M. A. Mahmud, and M. Farhadi-Kangarlu, "Non-linear integral higher-order sliding mode controller design for islanded operations of t-type three-phase inverter-interfaced distributed energy resources," *IET Generation, Transmission Distribution*, vol. 14, no. 1, pp. 53–61, 2020.

[23] M. A. Mahmud, H. R. Pota, and M. J. Hossain, "Nonlinear current control scheme for a single-phase grid-connected photovoltaic system," *IEEE Transactions on Sustainable Energy*, vol. 5, no. 1, pp. 218–227, 2014.

[24] Acil Allen Consulting Pty Ltd, "Regulatory Impact Statement: Bushfire Mitigation Regulations Ammendment," *Department of Economic Development, Jobs, Transport and Resources*, November 2015.

[25] M. A. Barik, A. Gargoom, M. A. Mahmud, M. E. Haque, H. Al-Khalidi, and A. M. Than Oo, "A decentralized fault detection technique for detecting single phase to ground faults in power distribution systems with resonant grounding," *IEEE Transactions on Power Delivery*, vol. 33, no. 5, pp. 2462–2473, 2018.